

1 *Type of the Paper (Article)*

## 2 **Spatial Variation in Canopy Structure across Forest** 3 **Landscapes**

4 **Brady S. Hardiman**<sup>1,2,\*</sup>, **Elizabeth A. LaRue**<sup>1</sup>, **Jeff W. Atkins**<sup>3</sup>, **Robert T. Fahey**<sup>4</sup>, **Franklin W.**  
5 **Wagner**<sup>1</sup>, **Chris M. Gough**<sup>3</sup>

6 <sup>1</sup>Dept. of Forestry & Natural Resources, Purdue University, 715 W. State Street, West Lafayette, IN 47907;  
7 bhardima@purdue.edu

8 <sup>2</sup>Dept. of Ecological and Environmental Engineering, Purdue University, 715 W. State Street, West Lafayette,  
9 IN 47907

10 <sup>3</sup>Dept. of Biology, Virginia Commonwealth University, 1000 W. Cary Street, Richmond, VA 23284;  
11 cmgough@vcu.edu

12 <sup>4</sup>Dept. of Natural Resources and the Environment and Center for Environmental Sciences and Engineering,  
13 University of Connecticut, 1376 Storrs Road, Storrs, CT 06269; robert.fahey@uconn.edu

14  
15 \* Correspondence: bhardima@purdue.edu; Tel.: +1-756-494-3593

16

17 **Abstract:** Forest canopy structure (CS) controls many ecosystem functions and is highly variable  
18 across landscapes, but the magnitude and scale of this variation is not well understood. We used a  
19 portable canopy lidar system to characterize variation in five categories of CS along  $N = 3$  transects  
20 (140–800 m long) at each of six forested landscapes within the eastern USA. The cumulative  
21 coefficient of variation was calculated for subsegments of each transect to determine the point of  
22 stability for individual CS metrics. We then quantified the scale at which CS is autocorrelated using  
23 Moran's  $I$  in an Incremental Autocorrelation analysis. All CS metrics reached stable values within  
24 300 m but varied substantially within and among forested landscapes. A stable point of 300 m for  
25 CS metrics corresponds with the spatial extent that many ecosystem functions are measured and  
26 modeled. Additionally, CS metrics were spatially autocorrelated at 40 to 88 m, suggesting that  
27 patch scale disturbance or environmental factors drive these patterns. Our study shows CS is  
28 heterogeneous across temperate forest landscapes at the scale of 10's of meters, requiring a  
29 resolution of this size for upscaling CS with remote sensing to large spatial scales.

30 **Keywords:** forest structure; macrosystems biology; portable canopy LiDAR; rugosity; transect  
31 spatial autocorrelation  
32

---

### 33 **1. Introduction**

34 In forested ecosystems, the density and spatial arrangement of vegetation, or canopy  
35 structure (CS), imposes strong controls on many scale-dependent ecosystem functions. CS in the  
36 form of leaf area and arrangement exerts a strong influence on forest production, through its effects  
37 on light absorption [1] and light-use efficiency [2,3]. CS metrics describing height and heterogeneity  
38 affect the turbulent exchange of gases between ecosystems and atmosphere, and regulate canopy  
39 net energy balance [4–6]. The spatial scale at which canopy structure exerts functionally meaningful

40 effects on ecosystem processes varies depending on forest type and architecture, environmental  
 41 factors, and the ecosystem functions and the CS element of interest. For example, patterns of light  
 42 transmittance relate to structure at the scale of individual leaves and small canopy gaps [7], while  
 43 boundary-layer processes are affected by gap to small landscape-scale canopy structure variation  
 44 [8]. Inferring and scaling ecosystem functions from remotely sensed measurements of forest  
 45 structure requires an understanding of how different measures of CS vary spatially across forested  
 46 landscapes.

47 CS is an emergent property of multiple underlying ecological factors operating at multiple  
 48 spatial scales [9–11]. Determinants of CS within landscapes may include at the smallest scales the  
 49 distribution of individual leaves owing to resource availability and at the landscape scale variation  
 50 in tree mortality and defoliation (Table 1) [12,13]. Additional within-landscape variation is  
 51 associated with the combined effects of individual-scale tree crown architecture, neighborhood-  
 52 scale community taxonomic diversity and competition, and environmental variables that shape  
 53 biomass production and allocation [14,15]. Variation within and among forest stands in these  
 54 canopy-shaping forces may determine the spatial scale at which CS stabilizes (i.e., spatial extent  
 55 within a stand at which heterogeneity in CS stabilizes), and the degree to which scales of stability  
 56 differ among forested landscapes [12]. Such understanding of the spatial scales and patterns of  
 57 variation in CS are essential precursors both to understanding the fundamental drivers of this  
 58 variation as well as to deriving, interpreting, and modeling ecosystem structure and function across  
 59 forest stands and landscapes.

60 Recent methodological advances in LiDAR have provided a means to better understand  
 61 spatial patterns in the variation of forest CS. Terrestrial LiDAR allows for a complete  
 62 characterization of the arrangement of vegetation throughout the entire canopy volume [16,17] with  
 63 a level of detail not possible with aerial or satellite forms of LiDAR [18]. Therefore, to advance our  
 64 understanding of the patterns in variation of forest CS, we choose to use terrestrial lidar to examine  
 65 and compare variation in landscape-scale CS of mature temperate forests in the northeastern, Great  
 66 Lakes, and prairie peninsula ecoclimatic domains of the USA (see Thorpe [19] for NEON domains).  
 67 We used terrestrial lidar to measure CS, which provides high resolution, spatially continuous  
 68 canopy structure data quantitatively describing vegetation density, arrangement, and heterogeneity  
 69 [20]. Our primary objective was to identify the magnitude of variation and spatial scale of stability  
 70 in CS within these forested landscapes. We focused on mature temperate forests to evaluate  
 71 whether these similarly-aged secondary forests located in the northern continental USA exhibit  
 72 similar spatial scales of CS stability.

73 **Table 1.** Examples of drivers and potential sources of spatial variation in canopy structure.

Driver	Literature source
Crown morphology/architecture	[21–25]
Disturbance	[26–32]
Demographics (community composition, diversity, succession)	[10,28,33–38]
Edaphic factors (topography, soil moisture, nutrient status, etc.)	[9,39–43]

## 75 2. Materials and Methods

### 76 2.1 Portable Canopy LiDAR and Forest Landscapes

77 We used a portable canopy LiDAR (PCL) system, a type of terrestrial LiDAR to survey CS  
78 along a vertical cross section of canopy. The portable canopy LiDAR system contains an upward  
79 facing, near-infrared pulsed laser operating at 2000Hz (Riegl LD90 3100 VHS; Riegl USA Inc.  
80 Orlando, Florida, USA) that is mounted to a frame worn by a user and operated along a transect at  
81 a constant speed. The design and operation of the instrument is outlined in Parker et al. [44]. Laser  
82 pulses emitted by the LiDAR unit either reflect off objects in the forest canopy or, when a gap is  
83 encountered, are not returned. These reflected and un-reflected pulses are recorded and used to  
84 construct a vertical cross-section of forest canopy. These “hit-grid” data (Fig. 1) are then used to  
85 calculate metrics of CS [2].

86 We collected PCL data from six deciduous forested landscapes in Eastern North America  
87 (Fig. 2). Five of the six landscapes were characterized by a deciduous, mixed hardwoods species  
88 composition, while Harvard Forest (HF) was composed primarily of eastern hemlock (*Tsuga*  
89 *Canadensis*). Within each landscape, we collected PCL data from  $N = 3$  transects (140 - 800 m; see Fig.  
90 S1 for individual transect lengths). We sampled within contiguous forest landscapes and thus  
91 sampling lengths varied among forested landscapes depending on the dimensions and area of each.  
92 Sampling after leaf-out occurred during May 2018 in Indiana locations at McCormick Creek (MCK),  
93 Lugar Farm (LUG), and Martell Forest (MTL); August 2017 at Harvard Forest (HF); during summer  
94 2016 at the University of Michigan Biological Station, and August 2017 at Hubbard Brook  
95 Experimental Forest (HBEF).

### 96 2.2 Canopy Structural Complexity

97 We focused our analysis on five metrics of CS broadly demonstrated to be functionally  
98 important, particularly with respect to canopy light interception and carbon uptake [1]. These  
99 metrics fall within five different CS categories: 1) vegetation height (mean maximum outer canopy  
100 height, MOCH); 2) vegetation density, volume, and area (mean vegetation area index, VAI); 3)  
101 arrangement and distribution (canopy rugosity,  $R_c$ ); 4) cover and openness (deep gap fraction, GF);  
102 and 5) vegetation variability (porosity, PC) [20]. The detailed definitions, derivation, and calculation  
103 of each of the 5 metrics are available in Atkins et al. [20]. The raw PCL data were processed using  
104 the *forestr* package [20], available in R 3.4.4 (R Core Team, 2018).

### 105 2.3 Statistical Analyses

106 Our first analysis identified the sampling distance at which CS metrics stabilized within each  
107 sampled forested landscape. Changes with sampling distance in the coefficient of variation (CV) of  
108 each CS metric was derived from cumulative 10-m means and variances across each transect (i.e. 0 -  
109 10, 0 - 20, 0 - 30, . . . up to the maximum transect length, varying from 140 - 800 m). The distances at  
110 which additional canopy structural information no longer significantly shifts in variance, hereafter  
111 termed “stability points”, were estimated from Bayesian changepoint analysis using the *bcp*  
112 package (Wang et al. 2015) in R 3.4.4 (R Core Team, 2018). The distance at which stability in the CV  
113 of CS metrics occurred was recorded using both methods and then averaged for a conservative

114 transect level measure of stability distance. We tested for differences in the mean stability point  
115 among forested landscapes for each CS metric with one-way ANOVAs. Stability points for Rc did  
116 not meet the assumption of normality, therefore we used a Kruskal-Wallis test to assess differences  
117 in mean stability points among forested landscapes. If the landscape effect was not significant, we  
118 calculated a mean stability point across forested landscape; if the effect was statistically significant,  
119 then we conducted post hoc Tukey tests to compare stability points among forested landscapes.

120 We conducted a second analysis with Incremental Autocorrelation analysis to assess spatial  
121 clustering patterns among CS metrics and across forested landscapes. For each forested landscape  
122 and CS metric combination we calculated Moran's  $I$  for all points separated by a given distance as a  
123 measure of autocorrelation by distance. We calculated the level of  $I$  at 10m distance increments for  
124 the full range of possible sampling distances, starting at 10m and ending at 150 (LUG, UMBS) or  
125 200m (all other sites). For each distance increment the  $z$ -score and  $p$ -value associated with the  
126 Moran's  $I$  test statistic were calculated and then  $z$ -scores were compared across distances. The  
127 distance (or distances) at which the  $z$ -score peaked was determined from the data and utilized as an  
128 indicator of spatial clustering for each metric and site combination. Incremental Autocorrelation  
129 analysis was conducted using the Spatial Analyst toolbox in ArcGIS v. 10.3 (ESRI; Redlands, CA,  
130 USA).

### 131 3. Results

#### 132 3.1 *Transect lengths at which CS metrics stabilize*

133 The stability points for two of the five CS metrics differed significantly among forested  
134 landscapes. Significant differences were observed among forested landscapes in the distance at  
135 which variation (i.e., as CV) in mean outer canopy height (Fig. 3A) and VAI (Fig. 3E) stabilized.  
136 Specifically, the stability point of mean outer canopy height for HF (262 m) was significantly greater  
137 than that of MLT (94 m) and MCK (92 m) (Fig. 3A). Additionally, the stability point for VAI at HF  
138 (241 m) was greater than that of LUG (87 m) and MCK (101 m). However, there were no significant  
139 differences in stability points among forested sites for gap fraction (Fig. 3B), canopy rugosity (Fig.  
140 3C), or porosity (Fig. 3D). Average stability points among forested landscapes for gap fraction,  
141 canopy rugosity, and porosity were 115 m, 125 m, and 144 m, respectively. All CS metrics exhibited  
142 a tendency to converge toward similar values at sufficiently long transect lengths (~300 m),  
143 regardless of site (Fig. S1). At all sites, CS metrics demonstrated sensitivity to putative ecotones or  
144 edaphic gradients as illustrated by sudden shifts in the value of their running mean (Fig. S2-5).

#### 145 3.2 *Scales of canopy structure autocorrelation*

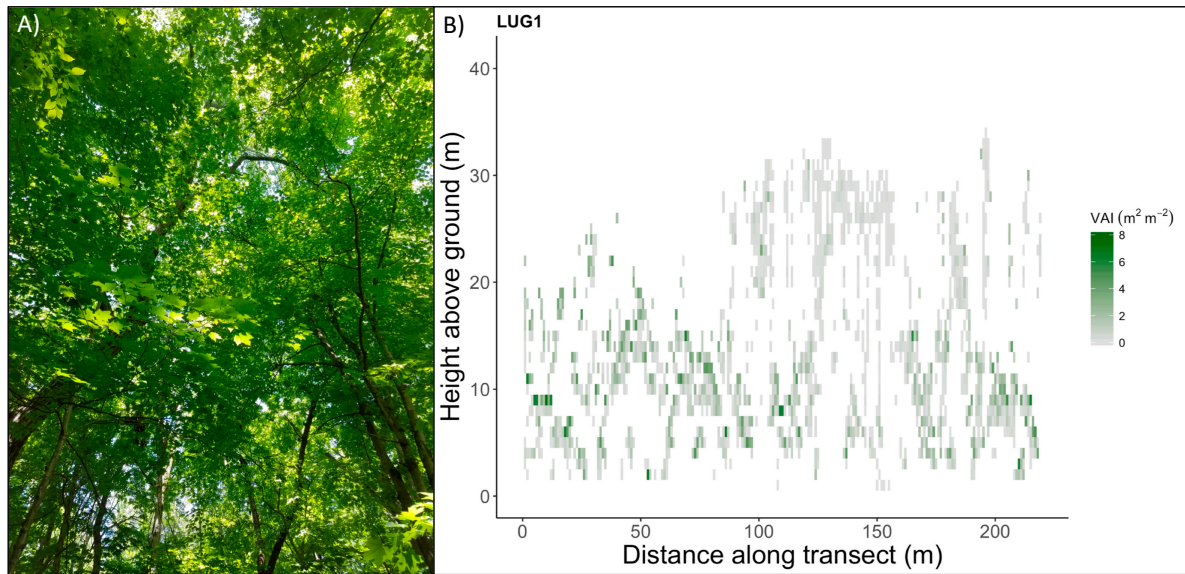
146 Peak spatial autocorrelation along transects varied among CS metrics and forested  
147 landscapes. Mean peak spatial autocorrelation distances of the five CS metrics varied substantially  
148 among CS metrics, ranging from 40 to 88 m (Table 2). Mean outer canopy height, VAI, and canopy  
149 rugosity displayed peak spatial autocorrelation at shorter distances than gap fraction and porosity  
150 (Table 2). While among forested landscapes, peak distances of spatial autocorrelation in CS metrics  
151 were highly variable, from 20 to 180 m (Table 2). For example, peak spatial autocorrelation of  
152 canopy rugosity ranged among landscapes from 20 to 150 m (mean = 53 m; Fig. 4), with MTL  
153 significantly peaking at both 30 and 150 m (Fig. 4). Similarly, VAI and porosity of MCK and mean  
154 out canopy height of MTL exhibited peak autocorrelation at multiple distances, indicating

155 correspondence of VAI at multiple spatial scales. Deep gap fraction, which was zero along many 10  
156 m transect subsegments, displayed significant peak autocorrelation distances in only two of six  
157 forested landscapes. One forested landscape, UMBS, exhibited a statistically significant peak  
158 distance of autocorrelation for porosity and canopy, but not for the other three CS metrics. Overall,  
159 peak autocorrelation when it occurred, varied substantially among forested landscapes for different  
160 CS metrics.

161 **Table 2.** Distance or distances (in meters) at which the z-score from Incremental Autocorrelation  
 162 analysis reached a statistically significant peak for canopy structural complexity metrics across six  
 163 forested landscapes in eastern USA. “---” indicates no significant peak was found in the data,  
 164 number in parentheses indicates the distance of the non-significant peak z-score on the curve if  
 165 there was one.

Site	MOCH	GF	R <sub>c</sub>	Porosity	VAI	Mean
UMBS	---	---	20	20	---	20
HEBF	30	50	20	40	150	58
HF	30	30	50	110	50	54
LUG	40	---	50	20	--- (70)	37
MCK	20	---	--- (80)	30/100	30/140	64
MTL	20/120	---	30/150	180	70	95
<b>Mean</b>	43	40	53	71	88	

MOCH: Mean Outer Canopy Height; GF: Gap Fraction;  
 R<sub>c</sub>: Canopy Rugosity; VAI: Vegetation Area Index

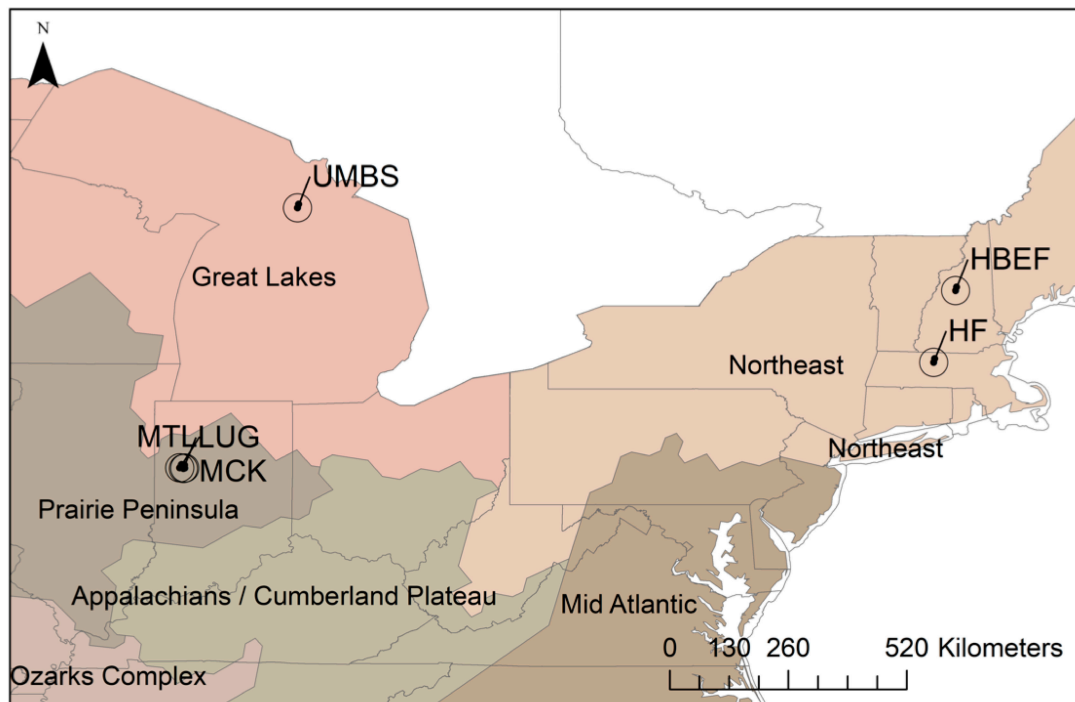


167

168

169 **Figure 1.** An example vertical cross section of a forest canopy collected from the portable canopy  
170 LiDAR. The transect was 250 m long and was collected within the Purdue University Lugar Farm  
171 Research Area, Indiana, USA. A) An image of the canopy at 0 m on the transect. B) Vegetation area  
172 index (VAI) was calculated using data collected along a 250 m transect with the portable canopy  
173 LiDAR unit. Each pixel in the cross section corresponds to a 1 m<sup>2</sup> bin containing values of VAI. The  
174 lighter to darker green shading corresponds to increasing values of VAI.

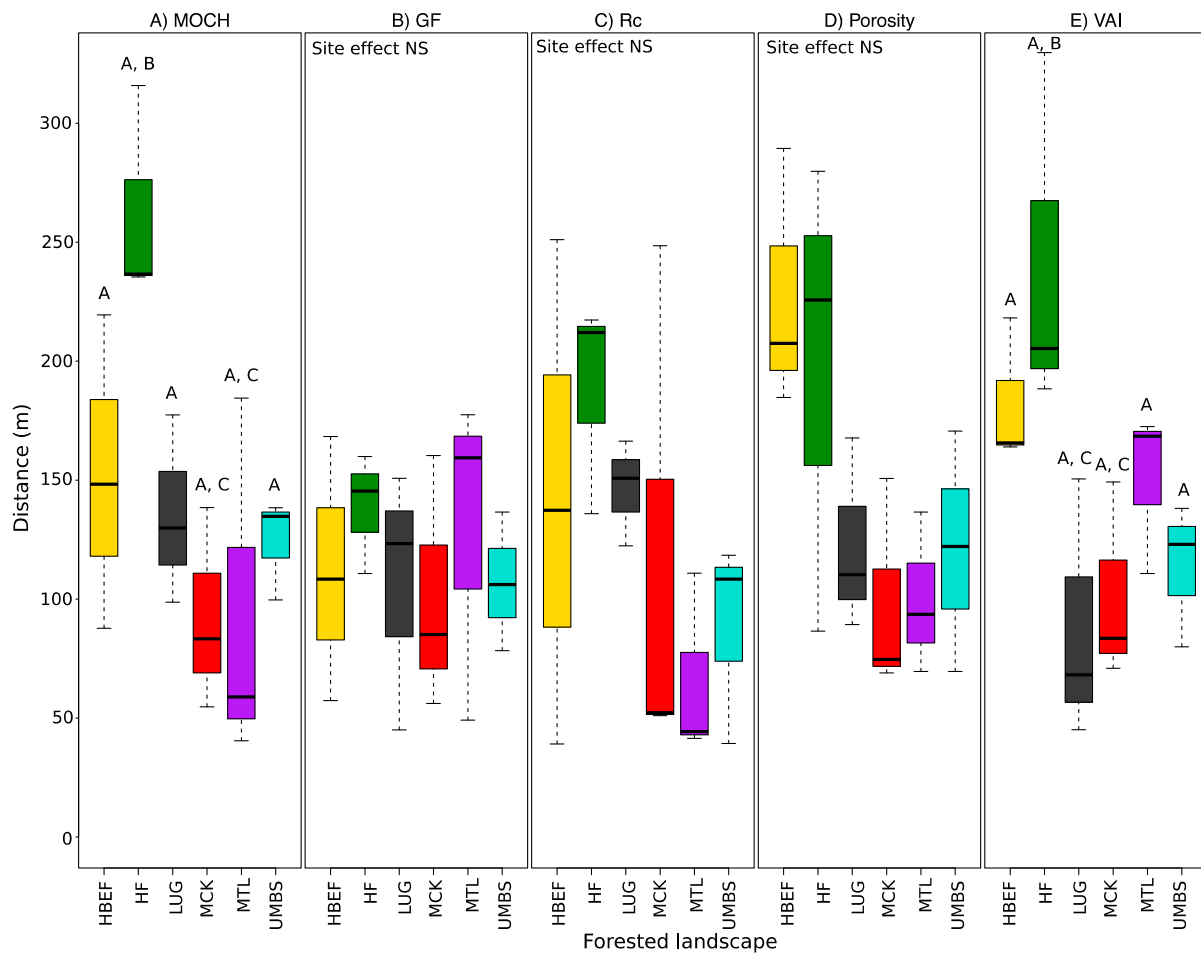
175



176

177 **Figure 2.** Sampling locations of the six forested landscapes for which portable canopy LiDAR data  
178 was collected in eastern USA. Martell Forest (MTL), McCormick Woods (MCK), and Lugar Farm  
179 (LUG) are located in the Prairie Peninsula ecoregion, Hubbard Brook (HBEF) and Harvard Forest  
180 Hemlock plot (HF) are in the Northeast ecoregion, and (UMBS) is in the Great Lakes forest  
181 ecoregion

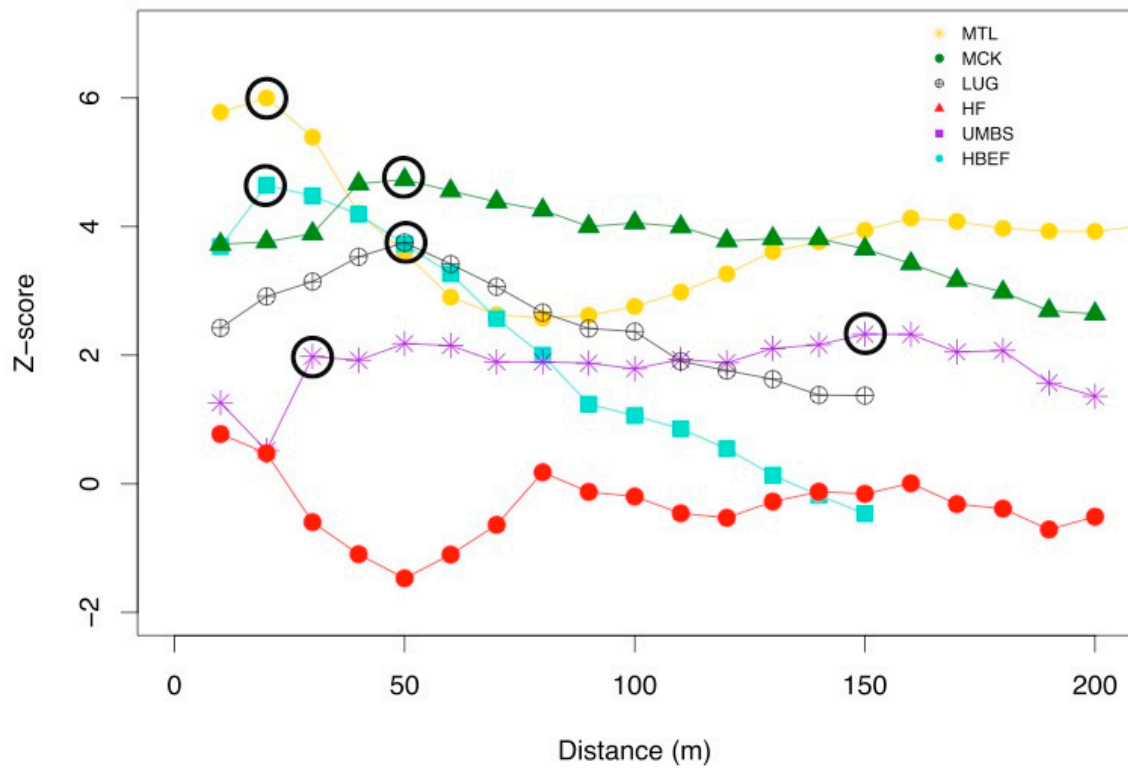
182



183

184 **Figure 3.** Estimated stability points of canopy structural complexity metrics from Bayesian  
 185 changepoint analysis along forested transects from six forested landscapes in eastern USA. CS  
 186 metrics included A) mean outer canopy height (MOCH;  $F_{5,12} = 4.31$ ,  $P = 0.01$ ), B) percentage of deep  
 187 gap fractions (GF;  $F_{5,12} = 0.26$ ,  $P = 0.92$ ), C) canopy rugosity (Rc;  $X^2 = 17$ ,  $P = 0.45$ ), D) porosity ( $F_{5,12} =$   
 188  $2.61$ ,  $P = 0.08$ ), and E) mean vegetation area index (VAI;  $F_{5,12} = 4.37$ ,  $P = 0.01$ ).  $N_{Transects} = 3$  per forested  
 189 landscape. Letters above bars indicate significantly different groups in post hoc Tukey tests if the  
 190 main effect of forested landscape in the univariate ANOVA or Kruskal-Wallis test was significant.

191



192

193 **Figure 4.** Peak spatial autocorrelation of canopy rugosity along transects from six forested  
 194 landscapes in eastern USA. The peak z-score from Incremental Autocorrelation analysis indicates  
 195 the distance at which spatial clustering of canopy rugosity is greatest along a transect. Circled  
 196 symbols indicate a statistically significant peak z-score for a forested landscape.  $N_{\text{Transects}} = 3$  per  
 197 forested landscape.  
 198

## 199 4. Discussion

### 200 4.1 Spatial variation and autocorrelation of canopy structure

201 CS varied substantially across spatial scales both within and among forest landscapes but,  
202 despite this variation, all CS metrics reached stable values within 300m. The distance at which CS  
203 stabilized varied substantially among forested landscapes, with midwestern sites generally  
204 achieved stability at shorter distances, suggesting greater structural homogeneity, than eastern  
205 sites. Among CS metrics, mean outer canopy height and VAI varied significantly among forested  
206 landscapes, while gap fraction, canopy rugosity, and porosity did not. Even so, all CS parameters  
207 and sites reached stability between 50 to 300 m indicating geographically and biologically distinct  
208 forested landscapes, and different measures of CS, reach stability at similar spatial scales of tens to  
209 hundreds of meters. This broad convergence of stability within 300 m shows that different  
210 structural measures within various landscapes align with many fundamental ecosystem functions  
211 that operate, and are measured and modeled at similar spatial scales, including net ecosystem  
212 production and evapotranspiration [4,45].

213 The spatial scale of CS autocorrelation suggests that the drivers creating this structure are  
214 likely to be local disturbance patterns or environmental quality. The mean spatial autocorrelation  
215 across forested landscapes ranged between 40 - 88 m. This local scale of spatial autocorrelation  
216 reveals the potential for landscape patterns of patchiness in CS features to emerge, with differences  
217 among landscapes occurring [46]. Such differences among metrics in spatial clustering likely reflect  
218 the underlying ecological drivers of each structural measure such as the variety in crown  
219 architecture and disturbance history in the specific forests that were sampled. For example, the CS  
220 metric with the shortest peak distance was gap fraction, which likely reflects the ubiquitous  
221 distribution of small gaps in the mature forest examined [47–49]. Likewise, VAI had the longest  
222 distance of peak autocorrelation, likely reflecting spatial differentiation within landscapes as a  
223 function of variable soil fertility and management history. For some CS metrics we observed a high  
224 degree of consistency across most or all forested landscapes (GF, Porosity, VAI) suggesting a  
225 common driver of these metrics, while the other metrics may be driven primarily by forest stand-  
226 specific factors such as recent disturbances. Indeed, forests at HF and HBEF have recently  
227 experienced well documented disruptions to CS prompted by widespread tree mortality [32,50,51].  
228 Accounting for this spatial autocorrelation in the design of a sampling plan can improve the  
229 robustness of studies that rely on the characterization of CS across space [52]. Our study clearly  
230 sheds light on the need to understand spatial scales of autocorrelation in CS, because the potential  
231 for patchiness in CS within and across landscapes will influence design of robust empirical studies  
232 and strategies for modeling forest processes.

233 While approaches to describing CS have become increasingly sophisticated with aerial  
234 LiDAR technologies, improving the understanding of how CS varies across spatial scales within  
235 stands, across landscapes, and among forest types may require the coupling of terrestrial and aerial  
236 LiDAR [53,54]. Our study shows that the spatial scale of stability in CS may be best characterized by  
237 terrestrial LiDAR, and then scaled up to a larger footprint with aerial LiDAR. Terrestrial LiDAR  
238 platforms provide an advantage over downward looking aerial LiDAR [18] by providing a  
239 characterization of the arrangement of canopy elements throughout the full canopy volume. CS  
240 metrics from terrestrial LiDAR have proven to have high value in describing structures that are

241 important to ecosystem functioning [1,55]. Similar information could be extracted from aerial  
242 LiDAR data, especially from full waveform or Geiger-mode platforms, but the correct scale at  
243 which to describe such CS metrics (which has generally been constrained in terrestrial LiDAR  
244 studies by sampling schemes) is not well understood. Recent studies have documented the  
245 substantial influence of CS, as measured by TLS, on remote sensing observations of forests (e.g.,  
246 Landsat; [56]), demonstrating potential new methods to derive additional information from existing  
247 data streams. However, despite these linkages, the spatial coherence of terrestrial and aerial  
248 measures of structure is uncertain due to differences in the scale of measurement. Coupling the two  
249 will require understanding of how stable or, conversely, variable CS metrics are within contiguous  
250 area of forestland.

#### 251 *4.2 Relevance to canopy structural scaling and modelling efforts*

252 Our results suggest that surveys of CS are likely to correspond well with functions  
253 examined at a 'foot-print' scale. For example, the maximum stability point of 300 m corresponds  
254 with the area of measurements of forest carbon exchange by eddy covariance towers [4,45].  
255 Analysis of stability points and autocorrelation scales for CS metrics indicate that CS can be  
256 robustly estimated and upscaled within an area of observation typical of that already employed by  
257 some forest ecological studies. While all metrics achieved stability within 300 m, some categories of  
258 CS metrics do appear inherently more spatially variable regardless of landscape (Fig. 3), suggesting  
259 that upscaling some metrics may necessitate coarser resolution of outputs. Given the spatial  
260 variation in stability points and auto-correlation across forest landscapes and parameters, scaling  
261 and modeling of CS requires a nuanced approach. Our analysis indicates that while CS is stable  
262 within landscapes, it tends to shift across landscapes, suggesting that scaling of contiguous  
263 landscape units may be important.

264 Improved characterization of spatial variation of CS has several potential benefits for  
265 understanding and modelling scale-dependent forest ecosystem processes. First, ecosystem models  
266 greatly simplify complex CS to improve computational tractability [57,58]. While computational  
267 tractability is desirable, output from such models often fails to accurately describe forest process  
268 and responses to disturbance [59]. More accurate representation of CS could improve model  
269 performance by increasing biological realism. Second, many ecosystem models accommodate some  
270 degree of vertical variation in vegetation distribution, but most do not explicitly incorporate  
271 horizontal heterogeneity in vertical variation, limiting their ability to accurately represent spatially  
272 heterogeneous processes such as disturbance events which are known to influence CS and functions  
273 such as carbon cycling [26,29]. Third, incorporating CS and the spatial variation thereof in  
274 ecosystem models offers opportunities to represent disturbance and successional changes through  
275 their effects on CS itself rather than by attempting to capture and represent the mechanism of  
276 disturbance itself.

## 277 **5. Conclusions**

278 We conclude that, although CS metrics stabilize within forested landscapes at different spatial  
279 scales, all approach stability at distances under 300 m. This is a range that is well aligned with the  
280 spatial scale at which many fundamental ecosystem functions are quantified using measurements  
281 and models. This finding has important implications for remote sensing, upscaling, and modeling

282 of CS and functions inferred from structure. New remote sensing platforms, such as terrestrial lidar,  
283 are increasingly available and are likely to become a common component of the forest ecology  
284 toolkit in the near future. The data generated by these tools will help to answer ecological questions  
285 requiring a rigorous understanding of the scales at which CS vary across the landscape.  
286 Furthermore, there are likely to be many drivers of landscape variation in canopy structure; future  
287 research should investigate the underlying causes of variation in CS across and within spatial  
288 scales.

289 **Supplementary Materials:** The following are available online at [www.mdpi.com/xxx/s1](http://www.mdpi.com/xxx/s1), Figure S1: Coefficient  
290 of variation of canopy structural complexity metrics from  $N=3$  individual transects at each of six forested  
291 landscapes in Eastern North America.

### 292 **Author Contributions:**

293 Conceptualization, Brady S. Hardiman and Jeff W. Atkins; Data curation, Jeff W. Atkins and  
294 Franklin W. Wagner; Formal analysis, Elizabeth A. LaRue, Jeff W. Atkins and Robert T. Fahey;  
295 Funding acquisition, Brady S. Hardiman, Robert T. Fahey and Christopher M. Gough;  
296 Methodology, Elizabeth A. LaRue, Jeff W. Atkins, Robert T. Fahey and Franklin W. Wagner; Project  
297 administration, Brady S. Hardiman, Robert T. Fahey and Christopher M. Gough; Resources, Brady  
298 S. Hardiman and Christopher M. Gough; Supervision, Brady S. Hardiman; Visualization, Elizabeth  
299 A. LaRue and Jeff W. Atkins; Writing – original draft, Brady S. Hardiman, Elizabeth A. LaRue, Jeff  
300 W. Atkins, Robert T. Fahey and Christopher M. Gough; Writing – review & editing, Brady S.  
301 Hardiman, Elizabeth A. LaRue, Jeff W. Atkins, Robert T. Fahey and Christopher M. Gough.

302 **Funding:** This research was funded by the National Science Foundation's Division of Emerging Frontiers,  
303 EAGER-NEON Awards 1550657 (to CMG), 1550650 (to RTF), and 1550639 (to BSH). CMG and JWA were  
304 additionally supported by National Science Foundation Award 1655095. EAL was supported in part by NSF  
305 Division of Emerging Frontiers Award 1638702 (to BSH).

306 **Acknowledgments:** We acknowledge the contributions of Michael Keller, Nathan Ibarluzea, Ke Xu, and Emily  
307 Summers who assisted with data collection at the Purdue University sites as well as Nat Cleavitt and Jackie  
308 Hatala-Matthes for assistance with data collection at Hubbard Brook Experimental Forest. We thank staff from  
309 the University of Michigan Biological Station, Harvard Forest, Hubbard Brook Experimental Forest, and  
310 Purdue University Department of Forestry and Natural Resources for material support.

311 **Conflicts of Interest:** The authors declare no conflict of interest.

### 312 **References**

- 313 1. Atkins, J. W.; Fahey, R. T.; Hardiman, B. S.; Gough, C. M. Forest Canopy Structural Complexity  
314 and Light Absorption Relationships at the Subcontinental Scale. *J. Geophys. Res. Biogeosciences* **2018**,  
315 *123*, 1387–1405.
- 316 2. Hardiman, B. S.; Bohrer, G.; Gough, C. M.; Vogel, C. S.; Curtis, P. S. The role of canopy structural  
317 complexity in wood net primary production of a maturing northern deciduous forest. *Ecology* **2011**,  
318 *92*, 1818–27.
- 319 3. Hardiman, B. S.; Gough, C. M.; Halperin, A.; Hofmeister, K. L.; Nave, L. E.; Bohrer, G.; Curtis, P.  
320 S. Maintaining high rates of carbon storage in old forests: A mechanism linking canopy structure to  
321 forest function. *For. Ecol. Manage.* **2013**, *298*, 111–119.

- 322 4. Maurer, K. D.; Hardiman, B. S.; Vogel, C. S.; Bohrer, G. Canopy-structure effects on surface  
323 roughness parameters: Observations in a Great Lakes mixed-deciduous forest. *Agric. For. Meteorol.*  
324 **2013**, *177*, 24–34.
- 325 5. Bonan, G. B. Forests and climate change: forcings, feedbacks, and the climate benefits of forests.  
326 *Science* **2008**, *320*, 1444–9.
- 327 6. Yang, R.; Friedl, M. A. Modeling the effects of three-dimensional vegetation structure on surface  
328 radiation and energy balance in boreal forests. *J. Geophys. Res.* **2003**, *108*, 8615.
- 329 7. Ellsworth, D. S.; Reich, P. B. Canopy structure and vertical patterns of photosynthesis and related  
330 leaf traits in a deciduous forest. *Oecologia* **1993**, *96*, 169–178.
- 331 8. Yang, R.; Friedl, M. A. Determination of roughness lengths for heat and momentum over boreal  
332 forests. *Boundary-Layer Meteorol.* **2003**, *107*, 581–603.
- 333 9. Aber, J. D.; Pastor, J.; Melillo, J. M. Changes in forest canopy structure along a site quality  
334 gradient in southern Wisconsin, USA. *Am. Midl. Nat.* **1982**, *108*, 256–265.
- 335 10. Parker, G. G.; Russ, M. E. The canopy surface and stand development: assessing forest canopy  
336 structure and complexity with near-surface altimetry. *For. Ecol. Manage.* **2004**, *189*, 307–315.
- 337 11. Hutchison, B. A.; Matt, D. R.; Mcmillen, R. T.; Gross, L. J.; Tajchman, S. J.; Norman, J. M. The  
338 Architecture of a Deciduous Forest Canopy in Eastern Tennessee, USA. *J. Ecol.* **1986**, *74*, 635–646.
- 339 12. Nadkarni, N. M.; McIntosh, A. C. S.; Cushing, J. B. A framework to categorize forest structure  
340 concepts. *For. Ecol. Manage.* **2008**, *256*, 872–882.
- 341 13. Kane, V. R.; Bakker, J. D.; McGaughey, R. J.; Lutz, J. a; Gersonde, R. F.; Franklin, J. F. Examining  
342 conifer canopy structural complexity across forest ages and elevations with LiDAR data. *Can. J. For.*  
343 *Res. Can. Rech. For.* **2010**, *40*, 774–787.
- 344 14. Ishii, H. T.; Tanabe, S.; Hiura, T. Exploring the relationships among canopy structure, stand  
345 productivity, and biodiversity of temperate forest ecosystems. *For. Sci.* **2004**, *50*, 342–355.
- 346 15. Lefsky, M. A.; Hudak, A. T.; Cohen, W. B.; Acker, S. A. Geographic variability in lidar  
347 predictions of forest stand structure in the Pacific Northwest. *Remote Sens. Environ.* **2005**, *95*, 532–  
348 548.
- 349 16. Paynter, I.; Saenz, E.; Genest, D.; Peri, F.; Erb, A.; Li, Z.; Wiggin, K.; Muir, J.; Raunonen, P.;  
350 Schaaf, E. S.; Strahler, A.; Schaaf, C. Observing ecosystems with lightweight, rapid-scanning  
351 terrestrial lidar scanners. *Remote Sens. Ecol. Conserv.* **2016**, *2*, 174–189.
- 352 17. Newnham, G. J.; Armston, J. D.; Calders, K.; Disney, M. I.; Lovell, J. L.; Schaaf, C. B.; Strahler, A.  
353 H.; Danson, F. M. Terrestrial Laser Scanning for Plot-Scale Forest Measurement. *Curr. For. Reports*  
354 **2015**, *1*, 239–251.

- 355 18. Kükenbrink, D.; Schneider, F. D.; Leiterer, R.; Schaepman, M. E.; Morsdorf, F. Quantification of  
356 hidden canopy volume of airborne laser scanning data using a voxel traversal algorithm. *Remote*  
357 *Sens. Environ.* **2017**, *194*, 424–436.
- 358 19. Thorpe, A. S.; Barnett, D. T.; Elmendorf, S. C.; Hinckley, E. L. S.; Hoekman, D.; Jones, K. D.;  
359 Levan, K. E.; Meier, C. L.; Stanish, L. F.; Thibault, K. M. Introduction to the sampling designs of the  
360 National Ecological Observatory Network Terrestrial Observation System. *Ecosphere* **2016**, *7*, 1–11.
- 361 20. Atkins, J.; Bohrer, G.; Fahey, R.; Hardiman, B.; Morin, T.; Stovall, A.; Zimmerman, N.; Gough, C.  
362 Quantifying forest and canopy structural complexity metrics from terrestrial LiDAR data using the  
363 *forestr* R package.
- 364 21. Niinemets, Ü. Photosynthesis and resource distribution through plant canopies. *Plant, Cell*  
365 *Environ.* **2007**, *30*, 1052–1071.
- 366 22. Mori, A.; Niinemets, Ü. Plant responses to heterogeneous environments: scaling from shoot  
367 modules and whole-plant functions to ecosystem processes. *Ecol. Res.* **2010**, *25*, 691–692.
- 368 23. Niinemets, Ü. A review of light interception in plant stands from leaf to canopy in different  
369 plant functional types and in species with varying shade tolerance. *Ecol. Res.* **2010**, *25*, 671–693.
- 370 24. Ishii, H.; Asano, S. The role of crown architecture, leaf phenology and photosynthetic activity in  
371 promoting complementary use of light among coexisting species in temperate forests. *Ecol. Res.*  
372 **2009**, *25*, 715–722.
- 373 25. Pretzsch, H.; Forrester, D. I.; Rötzer, T. Representation of species mixing in forest growth  
374 models: A review and perspective. *Ecol. Modell.* **2015**, *313*, 276–292.
- 375 26. Curtis, P. S.; Gough, C. M. Forest aging, disturbance and the carbon cycle. *New Phytol.* **2018**.
- 376 27. Franklin, J. Disturbances and structural development of natural forest ecosystems with  
377 silvicultural implications, using Douglas-fir forests as an example. *For. Ecol. Manage.* **2002**, *155*, 399–  
378 423.
- 379 28. Fotis, A. T.; Morin, T. H.; Fahey, R. T.; Hardiman, B. S.; Bohrer, G.; Curtis, P. S. Forest structure  
380 in space and time: Biotic and abiotic determinants of canopy complexity and their effects on net  
381 primary productivity. *Agric. For. Meteorol.* **2018**, *250–251*, 181–191.
- 382 29. Sagara, B. T.; Fahey, R. T.; Vogel, C. S.; Fotis, A. T.; Curtis, P. S.; Gough, C. M. Moderate  
383 disturbance has similar effects on production regardless of site quality and composition. *Forests*  
384 **2018**, *9*, 1–17.
- 385 30. Tanaka, H.; Nakashizuka, T. Fifteen years of canopy dynamics analyzed by aerial photographs  
386 in a temperate deciduous forest, Japan. *Ecology* **1997**, *78*, 612–620.
- 387 31. Hardiman, B. S.; Bohrer, G.; Gough, C. M.; Curtis, P. S. Canopy Structural Changes Following  
388 Widespread Mortality of Canopy Dominant Trees. *Forests* **2013**, *4*, 537–552.

- 389 32. Pederson, N.; Dyer, J. M.; Mcewan, R. W.; Hessler, A. E.; Mock, C. J.; Orwig, D. A.; Rieder, H. E.;  
390 Cook, B. I. The legacy of episodic climatic events in shaping temperate, broadleaf forests. *Ecol.*  
391 *Monogr.* **2014**, *84*, 599–620.
- 392 33. Fahey, R. T.; Alvareshere, B. C.; Burton, J. I.; D'Amato, A. W.; Dickinson, Y. L.; Keeton, W. S.; Kern,  
393 C. C.; Larson, A. J.; Palik, B. J.; Puettmann, K. J.; Saunders, M. R.; Webster, C. R.; Atkins, J. W.;  
394 Gough, C. M.; Hardiman, B. S. Shifting conceptions of complexity in forest management and  
395 silviculture. *For. Ecol. Manage.* **2018**, *421*, 59–71.
- 396 34. Hiroaki, T.; Van Pelt, R.; Parker, G.; Nadkarni, N. Age-related development of canopy structure  
397 and its ecological functions. In *Forest Canopies*; Lowman, M.; Rinker, H., Eds.; Elsevier Academic  
398 Press, 2004; pp. 102–117.
- 399 35. Fahey, R. T.; Fotis, A. T.; Woods, K. D. Quantifying canopy complexity and effects on  
400 productivity and resilience in late-successional hemlock-hardwood forests. *Ecol. Appl.* **2015**, *25*, 834–  
401 847.
- 402 36. McMahon, S. M.; Parker, G. G.; Miller, D. R. Evidence for a recent increase in forest growth. *Proc.*  
403 *Natl. Acad. Sci. U. S. A.* **2010**, *107*, 3611–3615.
- 404 37. Montgomery, R. A.; Chazdon, R. L. Forest structure, canopy architecture, and light  
405 transmittance in tropical wet forests. *Ecology* **2001**, *82*, 2707–2718.
- 406 38. McMahon, S. M.; Bebbler, D. P.; Butt, N.; Crockatt, M.; Kirby, K.; Parker, G. G.; Riutta, T.; Slade,  
407 E. M. Ground based LiDAR demonstrates the legacy of management history to canopy structure  
408 and composition across a fragmented temperate woodland. *For. Ecol. Manage.* **2015**, *335*, 255–260.
- 409 39. Nave, L. E.; Sparks, J. P.; Le Moine, J.; Hardiman, B. S.; Nadelhoffer, K. J.; Tallant, J. M.; Vogel, C.  
410 S.; Strahm, B. D.; Curtis, P. S. Changes in soil nitrogen cycling in a northern temperate forest  
411 ecosystem during succession. *Biogeochemistry* **2014**.
- 412 40. Morton, D. C.; Nagol, J.; Carabajal, C. C.; Rosette, J.; Palace, M.; Cook, B. D.; Vermote, E. F.;  
413 Harding, D. J.; North, P. R. J. Amazon forests maintain consistent canopy structure and greenness  
414 during the dry season. *Nature* **2014**, *506*, 1–16.
- 415 41. Saatchi, S.; Marlier, M.; Chazdon, R. L.; Clark, D. B.; Russell, A. E. Impact of spatial variability of  
416 tropical forest structure on radar estimation of aboveground biomass. *Remote Sens. Environ.* **2011**,  
417 *115*, 2836–2849.
- 418 42. Saatchi, S.; Asefi-Najafabady, S.; Malhi, Y.; Aragao, L. E. O. C.; Anderson, L. O.; Myneni, R. B.;  
419 Nemani, R. Persistent effects of a severe drought on Amazonian forest canopy. *Proc. Natl. Acad. Sci.*  
420 **2013**, *110*, 565–570.
- 421 43. Wirth, R.; Weber, B.; Ryel, R. J. Spatial and temporal variability of canopy structure in a tropical  
422 moist forest. *Acta Oecologica* **2001**, *22*, 235–244.
- 423 44. Parker, G. G.; Harding, D. J.; Berger, M. L. A portable LIDAR system for rapid determination of

- 424 forest canopy structure. *J. Appl. Ecol.* **2004**, *41*, 755–767.
- 425 45. Schmid, H. P.; Su, H. B.; Vogel, C. S.; Curtis, P. S. Ecosystem-atmosphere exchange of carbon  
426 dioxide over a mixed hardwood forest in northern lower Michigan. *J. Geophys. Res.* **2003**, *108*, 19.
- 427 46. Miller, T. F.; Mladenoff, D. J.; Clayton, M. K. Old-growth northern hardwood forests: spatial  
428 autocorrelation and pattern of understory vegetation. *Ecol. Monogr.* **2002**, *72*, 487–503.
- 429 47. Runkle, J. R. GAP REGENERATION IN SOME OLD-GROWTH FORESTS OF THE EASTERN-  
430 UNITED-STATES. *Ecology* **1981**, *62*, 1041–1051.
- 431 48. Runkle, J. R.; Yetter, T. C. Treefalls Revisited: Gap Dynamics in the Southern Appalachians.  
432 *Ecology* **1987**, *68*, 417–424.
- 433 49. HIBBS, D. E. GAP DYNAMICS IN A HEMLOCK HARDWOOD FOREST. *Can. J. For. Res. Can.*  
434 *Rech. For.* **1982**, *12*, 522–527.
- 435 50. Orwig, D. A.; Cobb, R. C.; D'Amato, A. W.; Kizlinski, M. L.; Foster, D. R. Multi-year ecosystem  
436 response to hemlock woolly adelgid infestation in southern New England forests. *Can. J. For. Res.*  
437 *Can. Rech. For.* **2008**, *38*, 834–843.
- 438 51. Orwig, D. A.; Barker Plotkin, A. A.; Davidson, E. A.; Lux, H.; Savage, K. E.; Ellison, A. M.  
439 Foundation species loss affects vegetation structure more than ecosystem function in a northeastern  
440 USA forest. *PeerJ* **2013**, *1*, e41.
- 441 52. Pickell, P. D.; Coops, N. C.; Gergel, S. E.; Andison, D. W.; Marshall, P. L. Evolution of Canada's  
442 boreal forest spatial patterns as seen from space. *PLoS One* **2016**, *11*, e0157736.
- 443 53. Schneider, F. D.; Leiterer, R.; Morsdorf, F.; Gastellu-Etchegorry, J. P.; Lauret, N.; Pfeifer, N.;  
444 Schaepman, M. E. Simulating imaging spectrometer data: 3D forest modeling based on LiDAR and  
445 in situ data. *Remote Sens. Environ.* **2014**, *152*, 235–250.
- 446 54. Moran, C. J.; Rowell, E. M.; Seielstad, C. A. A data-driven framework to identify and compare  
447 forest structure classes using LiDAR. *Remote Sens. Environ.* **2018**, *211*, 154–166.
- 448 55. Ehbrecht, M.; Schall, P.; Ammer, C.; Seidel, D. Quantifying stand structural complexity and its  
449 relationship with forest management, tree species diversity and microclimate. *Agric. For. Meteorol.*  
450 **2017**, *242*, 1–9.
- 451 56. LaRue, E.; Atkins, J.; Dahlin, K.; Fahey, R.; Fei, S.; Gough, C.; Hardiman, B. Linking Landsat to  
452 terrestrial LIDAR: Vegetation metrics of forest greenness are correlated with canopy structural  
453 complexity. *Int. J. Appl. Earth Obs. Geoinf.*
- 454 57. Mahadevan, P.; Wofsy, S. C.; Matross, D. M.; Xiao, X.; Dunn, A. L.; Lin, J. C.; Gerbig, C.; Munger,  
455 J. W.; Chow, V. Y.; Gottlieb, E. W. A satellite-based biosphere parameterization for net ecosystem  
456 CO<sub>2</sub> exchange: Vegetation Photosynthesis and Respiration Model (VPRM). *Global Biogeochem. Cycles*  
457 **2008**, *22*.

- 458 58. Medvigy, D.; Wofsy, S. C.; Munger, J. W.; Hollinger, D. Y.; Moorcroft, P. R. Mechanistic scaling  
459 of ecosystem function and dynamics in space and time: Ecosystem Demography model version 2. *J.*  
460 *Geophys. Res.* **2009**, *114*, 1–21.
- 461 59. Bond-Lamberty, B.; Fisk, J. P.; Holm, J. A.; Bailey, V.; Bohrer, G.; Gough, C. M. Moderate forest  
462 disturbance as a stringent test for gap and big-leaf models. *Biogeosciences* **2015**, *12*, 513–526.